Gait & Posture 37 (2013) 354–358

Contents lists available at SciVerse ScienceDirect

Gait & Posture

journal homepage: www.elsevier.com/locate/gaitpost

Estimation of spatio-temporal parameters for post-stroke hemiparetic gait using inertial sensors

Shuozhi Yang [a], Jun-Tian Zhang [a], Alison C. Novak [c], Brenda Brouwer [b,c], Qingguo Li [a,b,*]

[a] Department of Mechanical and Materials Engineering, Queen's University, Kingston, ON, Canada
[b] Human Mobility Research Centre, Queen's University and Kingston General Hospital, Kingston, ON, Canada
[c] School of Rehabilitation Therapy, Queen's University, Kingston, ON, Canada

ARTICLE INFO

Article history:
Received 31 December 2011
Received in revised form 27 May 2012
Accepted 31 July 2012

Keywords:
Walking speed
Hemiparetic gait
Spatio-temporal analysis
Inertial measurement unit
Stroke
Gait symmetry

ABSTRACT

This paper represents the first step in developing an inertial sensor system that is capable of assessing post-stroke gait in terms of walking speed and temporal gait symmetry. Two inertial sensors were attached at the midpoint of each shank to measure the accelerations and angular velocity during walking. Despite the abnormalities in hemiparetic gait, the angular velocity of most of the testing subjects (12 out of 13) exhibited similar characteristics as those from a healthy population, enabling walking speed estimation and gait event detection based on the pendulum walking model. The results from a standardized 10-meter walk test demonstrated that the IMU-based method has an excellent agreement with the clinically used stopwatch method. The gait symmetry results were comparable with previous studies. The gait segmentation failed when the angular velocity deviates significantly from the healthy groups' profile. With further development and concurrent validations, the inertial sensor-based system may eventually become a useful tool for continually monitoring spatio-temporal gait parameters post stroke in a natural environment.

1. Introduction

Stroke is a leading cause of adult disability in western countries [1]. According to World Health Organization estimates, 15 million people suffer from stroke each year, of which 5 million are permanently disabled [2]. Since gait impairments and mobility disorders can negatively impact independence, regaining community-based ambulatory mobility has been identified as a major rehabilitation goal for many stroke survivors [3]. Walking speed and gait symmetry have been widely used to evaluate post-stroke gait [4,5]. Self-selected walking speed has long been recognized as a proxy measure of ambulation quality and is used to quantify the progress of gait rehabilitation [6,7]. A widely accepted clinical assessment of short distance walking speed is the standardized 10-meter walk test (10 MWT) [8,9], which makes use of a stopwatch and the results reflect general physical function. On the other hand, temporal gait symmetry has been found as a significant predictor of hemiparetic walking performance and motor recovery [10,11]. Instrumented walkways (*e.g.*, the GAITRite system, CIR Systems Inc., NJ, USA), are commonly used to determine the temporal gait parameters, such as swing time and stance time of the paretic and nonparetic legs [12,11]. A limitation is that these systems are not typically available in clinical settings due to their size and cost. An inexpensive and easy-to-use system capable of assessing walking speed and gait symmetry simultaneously in a natural environment could be a cost-effective means for monitoring recovery during post-stroke rehabilitation.

Previous studies have demonstrated that miniature inertial sensors are well suited to evaluate the spatio-temporal parameters of human gait in activities of daily living. Inertial sensor based walking speed estimation methods have been developed and validated for healthy gait in the past several years [13–15]. Inertial sensors with more sophisticated strapdown algorithms have been developed for personal navigation applications as a potential alternative to the GPS system [16,17]. With the aid of the zero velocity update and Kalman filter, these systems were able to estimate the location of a pedestrian in a 3D indoor or outdoor environment [16,17]. Despite the progress in healthy gait and personal navigation, the use of inertial sensors in post-stroke hemiparetic gait analysis is mostly limited to the detection of gait events or counting steps [18,19].

Recently, triaxial ankle accelerometers combined with a machine learning algorithm have been used to recognize gait events and estimate walking speed in stroke survivors [20]. A limitation of this method is that subject-specific calibration using data collected from known distance walking at three different speeds over a known distance is required. The calibration

* Corresponding author at: Department of Mechanical and Materials Engineering, Queen's University, Kingston, ON, Canada. Tel.: +1 613 533 3191.
E-mail address: qli@me.queensu.ca (Q. Li).

0966-6362/$ – see front matter © 2012 Elsevier B.V. All rights reserved.
http://dx.doi.org/10.1016/j.gaitpost.2012.07.032

procedure is often performed in a clinical setting, which limits its generalizability to daily living environments. The objective of this study is to develop and evaluate an inertial sensor-based system that is capable of estimating walking speed and simultaneously evaluating gait symmetry for stroke survivors without the need of pre-calibration.

2. Methods

2.1. Apparatus

The Inertia-Link (MicroStrain, Inc., Williston, VT, USA) is an IMU sensor that consists of a triaxial accelerometer (±5 g, where g is the gravitational acceleration) and a triaxial gyroscope (±600°/s). Only two accelerometer axes and one gyroscope axis were used since we focused on the motion in the plane of progression (*i.e.*, sagittal plane). The accelerations and angular velocity data were collected at 100 Hz wirelessly.

2.2. Sensor configuration

Two IMU sensors were attached to the midpoint of each shank on the lateral side using athletic tape (Fig. 1). Before each experiment, subjects were asked to stand still with the shank vertical (longitudinal axis perpendicular to the floor) and the IMUs were adjusted such that the normal and tangential axes were aligned to vertical and horizontal directions of the global coordinate system, respectively.

2.3. Signal conditioning

Signal processing was performed using MATLAB (The MathWorks, Natick, MA, USA). In the gait event detection algorithm for the gait symmetry evaluation, a second-order Butterworth low-pass filter with a cut-off frequency of 10 Hz was used to remove noise from the raw angular velocity and acceleration measurements. For the gait segmentation, a second-order Butterworth low-pass filter with a cut-off frequency of 2.3 Hz was applied to the gyroscope signals.

2.4. Walking speed estimation

For each inertial sensor, the gait segmentation algorithm was implemented to divide a walking sequence into a series of stride cycles, and the average walking speed for each stride cycle was calculated for the paretic and non-paretic leg separately. The starting point of each stride cycle was defined as the shank vertical event, when the longitudinal direction of the shank was parallel to the direction of gravity. This specific gait event has been determined from the characteristics of the shank angular velocity (Fig. 2(a)) for healthy subjects [14]. Despite the differences in amplitude, the major characteristics (shape and peaks) of the angular velocities for both the paretic and non-paretic legs resemble the pattern of those of a healthy subject, as shown in Fig. 2(a) and (b). The similarity in features in the angular velocity profile enables the use of a single procedure segmentation of the gait cycle. The instantaneous shank velocities were calculated through direct time integration of the global coordinate accelerations, and then the walking speed was calculated for the corresponding stride cycle [14]. The use of gait segmentation did reduce the speed estimation error. However, further experiments identified that this method consistently underestimated walking speed [14]. To deal with this issue, an off-line linear regression-based calibration procedure was developed to correct the speed estimation error [15].

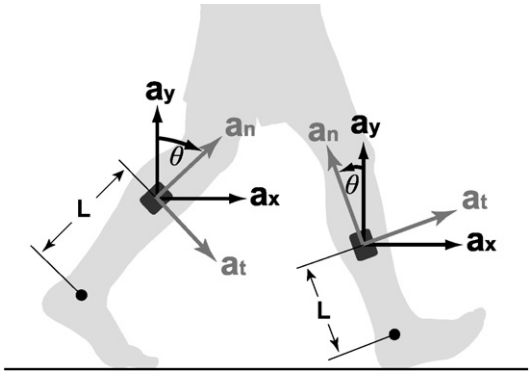

Fig. 1. Sensor configuration. An IMU is attached to the shank in the sagittal plane on the lateral side. Since only the shank motion in sagittal plane was considered in the method, the normal acceleration a_n is measured along the n direction, the tangential acceleration a_t is measured along the t direction, and the axis of the gyroscope is perpendicular to the sagittal plane defined by n and t directions. The arrows indicate positive axes for the corresponding sensor measurements. L is the sensor-to-ankle distance. The world coordinate system is defined by the x and y axes, and the vertical axis y extends in a direction parallel to gravity.

To eliminate the requirement of an off-line calibration, two new strategies were introduced to compensate the systematic error of speed under-estimation. First, the initial sensor velocity at the beginning of each stride cycle was taken into consideration. At the shank vertical event, although the shank angular velocity is minimal, it is not exactly zero (Fig. 2(b)). At the shank vertical event (when $\theta(0) = 0$), the initial sensor velocity is calculated as the product of the rotation radius and the rotation angular velocity,

$$v_t(0) = \omega(0) \cdot L \tag{1}$$

$$\begin{bmatrix} v_x(0) \\ v_y(0) \end{bmatrix} = \begin{bmatrix} \cos\theta(0) \\ -\sin\theta(0) \end{bmatrix} \cdot v_t(0) = \begin{bmatrix} v_t(0) \\ 0 \end{bmatrix}, \tag{2}$$

where $v_t(0)$ is the initial sensor velocity tangential to the shank. $v_x(0)$ and $v_y(0)$ are the initial sensor horizontal and vertical velocities in the global coordinate system, respectively. L is the distance from the sensor to the ankle joint (Lateral malleolus), which is approximately half of the total shank length (Fig. 1). These initial conditions, $v_x(0)$ and $v_y(0)$, are added to the calculation of instantaneous sensor velocities,

$$\begin{aligned} v'_x(t) &= \int_0^t a_x(\tau)d\tau + v_x(0) \\ v'_y(t) &= \int_0^t a_y(\tau)d\tau + v_y(0), \end{aligned} \tag{3}$$

where $v'_x(t)$ and $v'_y(t)$ are the instantaneous horizontal and vertical velocities obtained from integrating the sensor accelerations. a_x and a_y are the horizontal and vertical accelerations in the global coordinate system, transformed from the sensor accelerations, a_t and a_n (Fig. 1).

Second, the shank angular velocity measurements at the end of a stride cycle were used to correct the walking speed estimation error caused by the acceleration bias. The accelerometer measurement bias is inevitable for low-cost IMU sensors [21], and the direct consequence is velocity drift, resulting from the integration of biased acceleration data over a period of time. To determine the constant accelerometer bias, it requires a known reference velocity at the end of the stride cycle, calculated as the product of angular velocity, $\omega(T)$ and the rotation radius, L,

$$\begin{aligned} v_{xref}(T) &= \omega(T) \cdot L \\ v_{yref}(T) &= 0. \end{aligned} \tag{4}$$

Here we considered using the CABCS model [22], where the sensor error was modeled as a constant acceleration bias in the sensor coordinate system. By comparing these reference velocities with the sensor velocities calculated from integrating accelerations (Eq. (3)), the accelerometer biases in their sensitivity axes, a_{tbias} and a_{nbias}, were estimated. A detailed description can be found in Yang et al. [22].

With the estimated constant accelerometer bias, the velocity drifts were determined in a manner similar to the procedure shown in Eq. (3),

$$\begin{aligned} v_{xbias}(t) &= \int_0^t a_{xbias}(\tau)d\tau \\ v_{ybias}(t) &= \int_0^t a_{ybias}(\tau)d\tau, \end{aligned} \tag{5}$$

where $v_{xbias}(t)$ and $v_{ybias}(t)$ are the instantaneous horizontal and vertical velocity drifts due to the accelerometer measurement bias. a_{xbias} and a_{ybias} are the calculated horizontal and vertical acceleration bias in the global coordinate system, transformed from the accelerometer bias, a_{tbias} and a_{nbias}.

The corrected instantaneous velocities were calculated by removing the velocity drifts from the original instantaneous velocities of (Eq. (3)),

$$\begin{aligned} v_x(t) &= v'_x(t) - v_{xbias} \\ v_y(t) &= v'_y(t) - v_{ybias}, \end{aligned} \tag{6}$$

where $v_x(t)$ and $v_y(t)$ are the corrected instantaneous sensor horizontal and vertical velocities in global coordinate system, respectively.

After calculating the corrected instantaneous sensor velocities through Eqs. (1)–(6), the average velocities in the horizontal and vertical direction were calculated over a given stride cycle as

$$\begin{aligned} \overline{v}_x &= \frac{1}{T} \cdot \int_0^T v_x(t)dt \\ \overline{v}_y &= \frac{1}{T} \cdot \int_0^T v_y(t)dt, \end{aligned} \tag{7}$$

where $\overline{v}_x$ and $\overline{v}_y$ are the average horizontal and vertical velocities over the corresponding stride cycle in (0, T], as defined by gait segmentation.

The walking speed over the stride was then calculated as $\overline{v} = \sqrt{\overline{v}_x^2 + \overline{v}_y^2}$. This calculation helped to reduce the walking speed estimation errors resulted from minor misalignment of the accelerometer normal and tangential axes with the shank longitudinal and fore-aft directions. Using the walking speed per stride $\overline{v}$, the

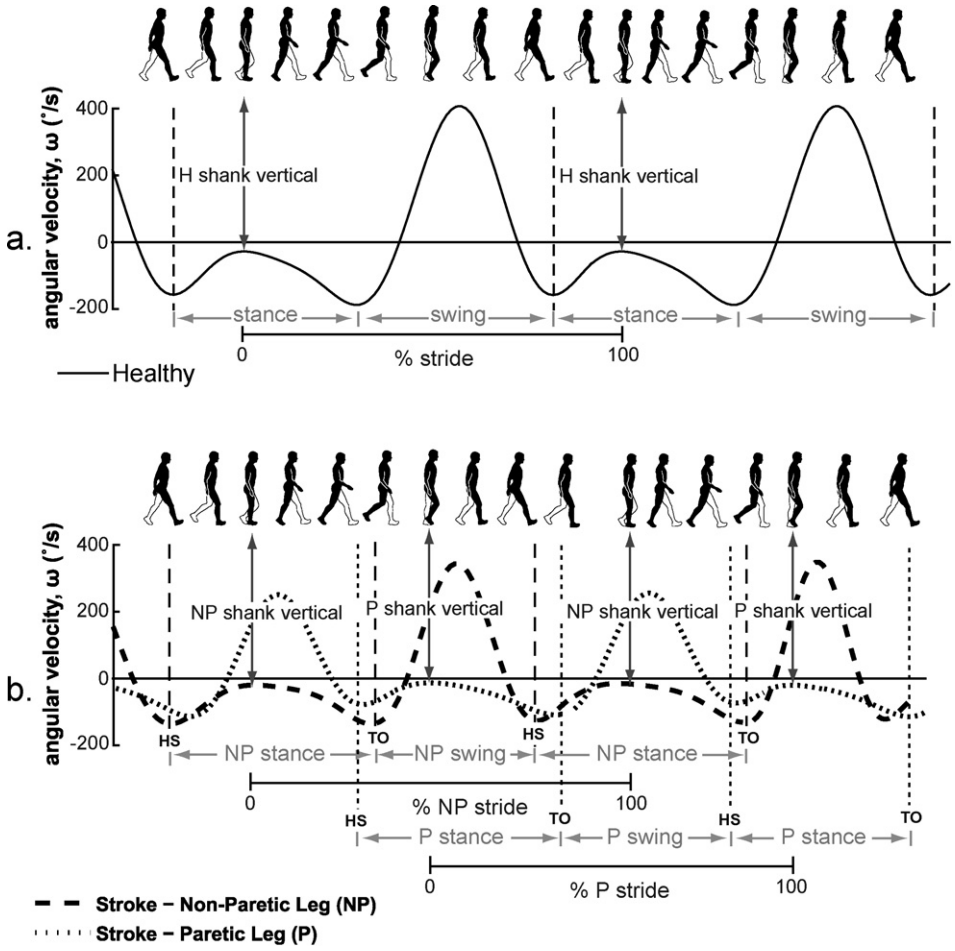

Fig. 2. Characteristic of shank angular velocity, ω, during two consecutive stride cycles. (a) Healthy subject and (b) Post-stroke subject. The angular velocity of the non-paretic leg (NP) is indicated by the thick dashed curve, and the paretic leg (P) is indicated by the thin dashed curve. The stride cycles of the NP leg and the P leg were determined by the mid-stance shank vertical event, at which point the magnitude of the angular velocity approached a local maximum close to zero. The swing phase and the stance phase of each leg were determined by the heel-strike (HS) and toe-off (TO) gait events, which were identified by the negative peaks of the shank angular velocity. The segmented stride cycles, the gait events and gait phases were labeled according to the aforementioned criteria.

mean walking speed over the 10-m walkway was calculated as the average of the individual stride speeds over the 10 m distance,

$$V_{IMU} = \frac{\sum_{i=1}^{N} \overline{v}(i)}{N} \tag{8}$$

where N is the total number of stride cycles in the 10-m walk. Two average walking speed estimates were obtained from sensors attached at the paretic and non-paretic limb separately.

2.5. Gait symmetry

The temporal parameters and phases of hemiparetic gait were determined based on the toe-off (TO) and the heel-strike (HS) gait events within a stride cycle. The swing phase time is the time difference between TO and the subsequent HS, and the stance phase is the rest of the stride cycle. A shank mounted gyroscope to detect these gait events has proven to be accurate and presents some advantages over foot mounted inertial sensors due to the simplicity of the detection algorithm [19,23]. The characteristics of the shank angular velocity and the gait phase definitions are shown in Fig. 2, where two negative peaks represent the TO and HS gait events [13,19,23]. The use of angular velocity for gait event detection reduced the complexity of the algorithm; however, the robustness for detecting gait events depends on the smoothness and the number of negative peaks of the filtered angular velocity signal. Marked deviations from the patterns illustrated in Fig. 2(b) may result in the false detection of TO and HS gait events and subsequently, errors in the gait symmetry calculation.

The swing phase and the stance phase of each stride were determined for the paretic and non-paretic leg separately. For each leg, the total stride cycle (T_{sc}) time is calculated as the sum of the stance time (T_{st}) and the swing time (T_{sw}). The percentage stance time ($\%T_{st}$) and the percentage swing time ($\%T_{sw}$) were calculated as $\%T_{st} = T_{st}/T_{sc} \times 100$ and $\%T_{sw} = T_{sw}/T_{sc} \times 100$, respectively. The following ratios for temporal symmetry were calculated as follows [11]: (1) Temporal swing ratio (R_{sw}) was defined as the ratio between the paretic swing time ($T_{sw}(P)$) and the non-paretic swing time ($T_{sw}(NP)$). (2) Temporal stance ratio R_{st} was defined as the ratio between the paretic stance time ($T_{st}(P)$) and the non-paretic stance time ($T_{st}(NP)$). (3) Temporal swing-stance ratio (SSR) was defined as the ratio between the stance time and the swing time (for each limb: paretic and non-paretic). (4) Overall temporal symmetry ratio was defined as the ratio between the paretic swing-stance ratio and the non-paretic swing-stance ratio. For a perfect symmetric gait, temporal swing ratio (R_{sw}), temporal stance ratio (R_{st}) and overall temporal symmetry ratio will equal one. Normal symmetry was defined as falling within ± 0.05 of unity for stance and swing and ± 0.10 of unity for overall symmetry [11].

2.6. Experimental method

2.6.1. Subjects

Thirteen subjects with stroke were recruited from the community forming a sample of convenience including ten males and three females (age: 59.5 ± 10.3 years; height: 168.1 ± 8.1 cm; weight: 73.7 ± 16.1 kg; shank length: 37.0 ± 2.2 cm; time post-stroke: 23.4 ± 15.1 months). Eight had left hemiparesis and five had right hemiparesis. All were screened to ensure they: (1) reported residual unilateral lower limb weakness, (2) were able to walk independently, and (3) could follow instructions. All subjects gave their informed consent to participate, and the study protocol was approved by the Research Ethics Board of the university.

2.6.2. Protocol

Subjects were instructed to walk three times at their self-selected speed along a straight hallway with yellow adhesive tape marking a 10-m distance on the floor. The reference walking speed for each trial in m/s was calculated by dividing the distance (10 m) by the recorded time by a stopwatch.

2.7. Data analysis

The Bland–Altman method [24] was used to compare the walking speed measured with a stopwatch to that estimated by the IMU method. The mean of the differences and ±2 standard deviations (SD) across all trials were plotted to illustrate the bias and the limits of agreement between the two methods.

Student's *t*-tests were applied to examine the significance of differences of the percentage stance time ($\%T_{st}$) and the percentage swing time ($\%T_{sw}$) between the non-paretic and paretic legs, with $p < 0.05$ indicating statistical significance. For the temporal symmetry measurements, it was determined whether the ratios differed from unity.

3. Results

Data from 12 subjects were included in the walking speed estimation analysis and gait symmetry analysis. One subject's data was excluded due to the inability of the algorithm to detect the gait events correctly (see Section 4). The mean self-selected 10 MWT speed (±1SD) was 0.93 ± 0.20 m/s, which is comparable to other studies investigating people with stroke with mild to moderate impairment [12,18,25]. Strong agreement between the walking speed estimated from the IMU sensors and the reference walking speed obtained using a stopwatch was clearly evident. The mean difference was 0.01 m/s with limits of agreement from −0.07 to 0.09 m/s for the non-paretic leg (Fig. 3(a)). Similarly, for the paretic leg, the mean difference was 0.00 m/s with limits of agreement from −0.09 to 0.09 m/s (Fig. 3(b)).

The percentage of the stride spent in swing and stance were significantly different between the paretic leg ($\%T_{sw}$ = 46.72± 3.70 %; $\%T_{st}$ = 53.28± 3.70 %) and the non-paretic leg ($\%T_{sw}$ = 40.54± 2.86 %; $\%T_{st}$ = 59.46± 2.86 %); $p < 0.05$). The swing/stance ratios (*SSR*) were SSR_{NP} = 0.69 ± 0.08 for the non-paretic leg and SSR_P = 0.89 ± 0.14 for the paretic leg. The temporal swing ratio and the temporal stance ratio were R_{sw} = 1.16 ± 0.11 and R_{st} = 0.90 ± 0.07, respectively. The overall temporal symmetry, calculated as a ratio between SSR_P and SSR_{NP}, was 1.30 ± 0.24. All differed from 1.0 reflecting asymmetry.

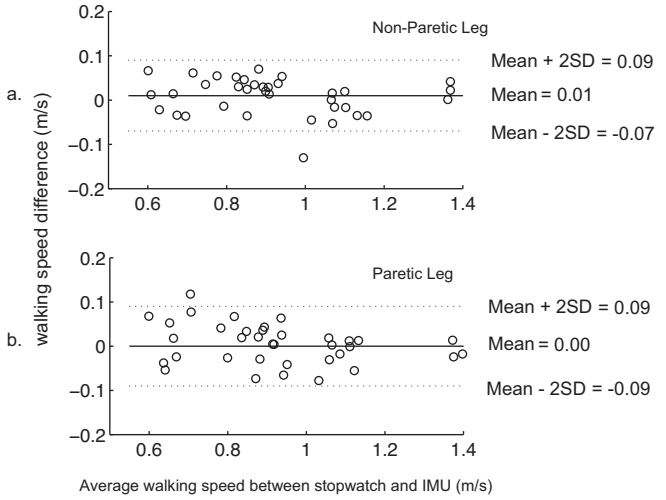

Fig. 3. Bland–Altman plots for walking speed measured by the stopwatch and IMUs (a. Non-paretic leg and b. Paretic leg). The *x*-axis depicts the average walking speed (m/s) determined from the IMU sensor and stopwatch, and the *y*-axis depicts the difference between these two methods. Each circle represents one data point from a single walking trial. The solid lines indicate the overall mean of the measurement difference, and the dashed lines show the limits of agreement (±2SD).

4. Discussion

For our study sample very small biases (non-paretic leg: 0.01 m/s; paretic leg: 0.00 m/s) were found(Fig. 3(a) and (b)), thus confirming that the algorithm did not require an offset adjustment or off-line calibration. The differences in walking speed measured using a stopwatch and from the IMUs were less than 0.09 m/s for the sensor on the paretic leg and 0.08 m/s for sensor on the non-paretic leg (at 95% probability). For context, walking speed measured by stopwatch compares well with an infrared timing gate (ITG) system revealing a difference of 0.01 m/s in the 10 MWT performed by subjects with traumatic brain injury [26]. The discrepancies detected in the current study were greater, however not likely of clinical relevance. Recent studies have reported that changes in stroke gait beyond 0.16 m/s [27] or 0.175 m/s [28]) are functionally meaningful. Our data indicated that the IMU-based algorithm used here produced estimates that are sufficiently in determining functionally meaningful changes in stroke gait.

For all but one subject tested (12 of 13), the patterns of shank angular velocity were consistent and the profiles were similar to the healthy population (Fig. 2). When the shank angular velocity characteristics deviated both from the healthy group profile and the typical stroke profile, the gait segmentation algorithm failed (Fig. 4). Observationally, this subject walked with a "stiff" gait with the knee held in extension throughout stance, which would limit push-off and reduce hip flexion [29]. The subject was the slowest walker with an average walking speed of 0.53 m/s, suggesting greater functional impairment than others. The oscillation in shank angular velocity counters the assumptions of the model suggesting that new gait segmentation methods need to be developed. A possible solution is to incorporate acceleration measurements to determine key gait events and sensor orientation. Further algorithm development and testing must also consider more seriously affected subjects who walk at speeds below 0.6 m/s [30].

Gait symmetry measurements obtained with IMUs revealed temporal asymmetry in terms of swing ratio (R_{sw}), stance ratio (R_{st}) and overall symmetry ratio, consistent with symmetry measures reported in subjects with mild impairment due to stroke

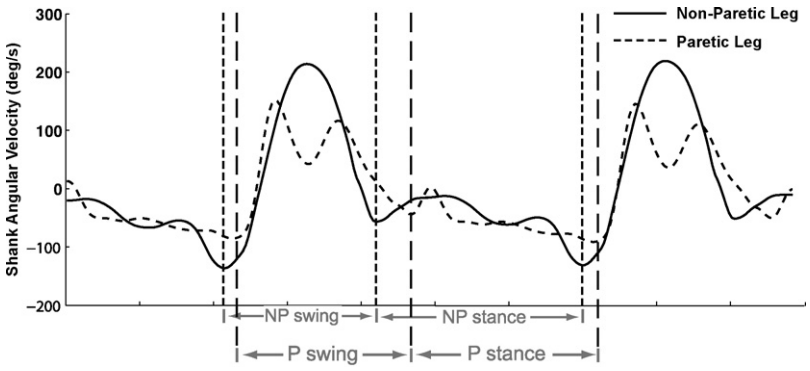

Fig. 4. Shank angular velocity profile for a subject who walks slower than 0.6 m/s. Multiple negative peaks in the angular velocities prevented the algorithm from correctly identifying key gait events.

(1.17 ± 0.05, 0.91 ± 0.02, and 1.29 ± 0.07, respectively) [11]. Shank-mounted gyroscopes have been shown to outperform other combinations of sensor types and mounting locations yielding the highest performance index (mean value) for determining toe-off and heel-strike events [19]. The current findings support the validity of a shank-mounted gyroscope for quantifying temporal gait symmetry. However, concurrent validation with a laboratory-based motion capture system serving as the gold standard would be useful to confirm the accuracy of our algorithm.

This study represents the first step in developing an integrated system that is capable of assessing walking speed and temporal symmetry in stroke gait. The current method improves on previous methods [14,20] is that the current method effectively estimates walking speed and determines temporal gait symmetry without the need for a population-based calibration prior gait assessment. With a stand-alone implementation, it provides a viable solution to assessing spatio-temporal gait in a natural environment.

Conflict of interest statement

No author of this paper has a conflict of interest, including specific financial interests, relationships, and/or affiliations relevant to the subject matter or materials included in this manuscript.

References

[1] Khaw K. Epidemiology of stroke. Journal of Neurology Neurosurgery and Psychiatry 1996;61(4):333–8.
[2] Mackay J, Mensah GA, Mendis S, Greenlund K. The atlas of heart disease and stroke. World Health Organization; 2004.
[3] Richards CL, Olney SJ. Hemiparetic gait following stroke. Part II: Recovery and physical therapy. Gait & Posture 1996;4(2):149–62.
[4] Hesse S. Rehabilitation of gait after stroke: evaluation, principles of therapy, novel treatment approaches, and assistive devices. Topics in Geriatric Rehabilitation 2003;19(2):109–26.
[5] Woolley SM. Characteristics of gait in hemiplegia. Topics in Stroke Rehabilitation 2001;7(4):1–18.
[6] Richards C, Malouin F, Dumas F, Tardif D. Gait velocity as an outcome measure of locomotor recovery after stroke. In: Gait analysis: theory and application. St. Louis, MO: Mosby; 1995. p. 355–64.
[7] Mudge S, Stott NS. Outcome measures to assess walking ability following stroke: a systematic review of the literature. Physiotherapy 2007;93(3):189–200.
[8] Salbach NM, Mayo NE, Higgins J, Ahmed S, Finch LE, Richards CL. Responsiveness and predictability of gait speed and other disability measures in acute stroke. Archives of Physical Medicine and Rehabilitation 2001;82(9):1204–12.
[9] Jorgensen JR, Bech-Pedersen DT, Zeeman P, Sorensen J, Andersen LL, Schonberger M. Effect of intensive outpatient physical training on gait performance and cardiovascular health in people with hemiparesis after stroke. Physical Therapy 2010;90(4):527–37.
[10] Olney SJ, Richards C. Hemiparetic gait following stroke. Part I: Characteristics. Gait & Posture 1996;4(2):136–48.
[11] Patterson KK, Parafianowicz I, Danells CJ, Closson V, Verrier MC, Staines WR, et al. Gait asymmetry in community-ambulating stroke survivors. Archives of Physical Medicine and Rehabilitation 2008;89(2):304–10.
[12] Balasubramanian CK, Bowden MG, Neptune RR, Kautz SA. Relationship between step length asymmetry and walking performance in subjects with chronic hemiparesis. Archives of Physical Medicine and Rehabilitation 2007;88(1):43–9.
[13] Aminian K, Najafi B, Bula C, Leyvraz PF, Robert P. Spatio-temporal parameters of gait measured by an ambulatory system using miniature gyroscopes. Journal of Biomechanics 2002;35(5):689–99.
[14] Li Q, Young M, Naing V, Donelan JM. Walking speed estimation using a shank-mounted inertial measurement unit. Journal of Biomechanics 2010;43(8):1640–3.
[15] Yang S, Li Q. IMU-based ambulatory walking speed estimation in constrained treadmill and overground walking. Computer Methods in Biomechanics and Biomedical Engineering 2011;15(3):313–22.
[16] Foxlin E. Pedestrian tracking with shoe-mounted inertial sensors. Computer Graphics and Applications IEEE 2005;25(6):38–46.
[17] Ojeda L, Borenstein J. Non-GPS navigation for security personnel and first responders. Journal of Navigation 2007;60(03):391–407.
[18] Mizuike C, Ohgi S, Morita S. Analysis of stroke patient walking dynamics using a tri-axial accelerometer. Gait & Posture 2009;30:60–4.
[19] Lau H, Tong K. The reliability of using accelerometer and gyroscope for gait event identification on persons with dropped foot. Gait & Posture 2008;27(2):248–57.
[20] Dobkin BH, Xu X, Batalin M, Thomas S, Kaiser W. Reliability and validity of bilateral ankle accelerometer algorithms for activity recognition and walking speed after stroke. Stroke 2011;42(8):2246–50.
[21] Thong Y, Woolfson M, Crowe J, Hayes-Gill B, Challis R. Dependence of inertial measurements of distance on accelerometer noise. Measurement Science and Technology 2002;13:1163–72.
[22] Yang S, Laudanski A, Li Q. Inertial sensors in estimating walking speed and inclination: an evaluation of sensor error models. Medical and Biological Engineering and Computing 2012;50(4):383–93.
[23] Catalfamo P, Ghoussayni S, Ewins D. Gait event detection on level ground and incline walking using a rate gyroscope. Sensors 2010;10(6):5683–702.
[24] Bland JM, Altman DG. Statistical methods for assessing agreement between two methods of clinical measurement. International Journal of Nursing Studies 2010;47(8):931–6.
[25] von Schroeder HP, Coutts RD, Lyden PD, Billings Jr E, Nickel VL. Gait parameters following stroke: a practical assessment. Journal of Rehabilitation Research and Development 1995;32(1):25–31.
[26] Van Loo M, Moseley A, Bosman J, de Bie R, Hassett L. Inter-rater reliability and concurrent validity of walking speed measurement after traumatic brain injury. Clinical rehabilitation 2003;17(7):775–9.
[27] Tilson JK, Sullivan KJ, Cen SY, Rose DK, Koradia CH, Azen SP, et al. Meaningful gait speed improvement during the first 60 days poststroke: minimal clinically important difference. Physical Therapy 2010;90(2):196–208.
[28] Fulk GD, Ludwig M, Dunning K, Golden S, Boyne P, West T. Estimating clinically important change in gait speed in people with stroke undergoing outpatient rehabilitation. Journal of Neurologic Physical Therapy 2011;35(2):82–9.
[29] Olney SJ. Training gait after stroke: a biomechanical perspective. In: Refshauge K, Ada L, Ellis E, editors. Science-based rehabilitation theories into practice. Oxford: Elsevier; 2005. p. 159–84.
[30] Olney SJ, Griffin MP, Monga TN, MacBride ID. Work and power in gait of stroke patients. Archives of Physical Medicine and Rehabilitation 1991;72(5):309–14.